



# Bending of Shear Deformable Plates Resting on Winkler Foundations According to Trigonometric Plate Theory

Atteshamuddin S. Sayyad<sup>1</sup>, Yuwaraj M. Ghugal<sup>2</sup>

<sup>1</sup> Department of Civil Engineering, SRES's Sanjivani College of Engineering, Savitribai Phule Pune University, Kopergaon-423601, Maharashtra, India  
Email: attu\_sayyad@yahoo.co.in,

<sup>2</sup> Department of Applied Mechanics, Government College of Engineering, Karad-415124, Shivaji University, Kolhapur, Maharashtra State, India  
Email: ghugal@rediffmail.com

Received August 20 2017; Revised October 01 2017; Accepted for publication October 19 2017.

Corresponding author: Atteshamuddin S. Sayyad, attu\_sayyad@yahoo.co.in

Copyright © 2018 Shahid Chamran University of Ahvaz. All rights reserved.

**Abstract.** A trigonometric plate theory is assessed for the static bending analysis of plates resting on Winkler elastic foundation. The theory considers the effects of transverse shear and normal strains. The theory accounts for realistic variation of the transverse shear stress through the thickness and satisfies the traction free conditions at the top and bottom surfaces of the plate without using shear correction factors. The governing equations of equilibrium and the associated boundary conditions of the theory are obtained using the principle of virtual work. A closed-form solution is obtained using double trigonometric series. The numerical results are obtained for flexure of simply supported plates subjected to various static loadings. The displacements and stresses are obtained for three different values of foundation modulus. The numerical results are also generated using higher order shear deformation theory of Reddy, first order shear deformation theory of Mindlin, and classical plate theory for the comparison of the present results.

**Keywords:** Shear deformation; Normal strain; Shear stress; Shear correction factor; Winkler elastic foundation; Foundation modulus.

## 1. Introduction

The bending of plates resting on elastic foundation has many practical applications in civil, mechanical, aerospace, marine, offshore, and automotive structures. Therefore, various analytical and numerical methods have been employed to study bending analysis of plates resting on elastic foundation. Winkler foundation is the most commonly used elastic foundation. The well-known classical plate theory (CPT) is based on the Kirchhoff [1] hypothesis that straight lines perpendicular to the midplane before deformation remain straight and perpendicular to the midplane after deformation. The theory assumes linear variation of inplane displacements through the thickness and neglects the effects of transverse shear deformation and normal strain. In the Mindlin [2] first-order shear deformable theory (FSDT), it is assumed that straight lines perpendicular to the mid-surface before deformation remain straight but not perpendicular to the mid-surface after deformation. The theory removes some of the defects of the classical plate theory. Although this theory considers the effect of transverse shear deformation, it neglects the effect of transverse normal strain. Although the effect of transverse shear deformation is considered in this theory, the effect of transverse normal strain is neglected. This theory predicts the constant shear strain through the plate thickness and requires a problem dependent shear correction coefficient. These limitations of CPT and FSDT have been rectified in recent years by introducing higher-order functions in the displacement field which has led to the development of higher-order plate theories. The third order theory of Reddy [3] is a well-known higher order theory but neglects the effect of transverse normal



strain. Matsunaga [4] obtained natural frequencies and buckling stresses of a thick isotropic plate resting on two-parameter elastic foundations considering the effect of shear deformation, thickness change, and rotatory inertia. A higher order theory based on power series expansion of the displacement components is used. The bending analysis of a plate resting on Winkler elastic foundation is studied by Huang and Thambiratnam [5]. Chen and Bian [6] applied the methods of state space and the differential quadrature for bending and free vibration of arbitrarily thick beams resting on a Pasternak elastic foundation. A new shear deformation theory for the free vibration analysis of simply supported functionally graded plates resting on a Winkler-Pasternak elastic foundation has been presented by Atmane et al. [7]. The closed-form solutions were obtained by using Navier technique. Thai et al. [8] proposed a refined shear deformation theory for bending, buckling, and vibration of thick plates resting on elastic foundation. The elastic foundation is modeled as two-parameter Pasternak foundation. The Levy-type solution is presented for rectangular plates with two opposite simply-supported edges and the other two edges having arbitrary boundary conditions. Zenkour [9] carried out bending analysis of orthotropic plates resting on Pasternak's foundations by using the mixed first-order shear deformation theory. Zenkour et al. [10] also presented mixed first-order theories for plates resting on elastic foundations. Sayyad [11] has developed the exponential shear deformation theory for the bending of orthotropic plates. Akbas [12] presented free vibration and static bending of a simply-supported functionally graded plate with the porosity effect using the first-order shear deformation theory. Akbas [13, 14] also presented static and stability analysis of a nanoplate using the generalized differential quadrature method based on the classical plate model. Civalek [15] and Gurses et al. [16, 17] developed the discrete singular convolution method, for the static analysis of thick symmetric cross-ply laminated composite plates based on the first-order shear deformation theory. Recently, Sayyad and Ghugal [18, 19] presented a detailed review of displacement-based shear deformation theories for the analysis of beams and plates.

### 1.1. Motivation and contribution

1. It is highly recommended that any refinements of classical models are meaningless in general, unless the effects of transverse shear and normal deformations are both taken into account. But, in a whole lot of literature on this subject many researchers neglected this effect in view of minimizing the number of unknown variables. In the present study, authors have developed a trigonometric shear deformation theory for the bending of shear flexible plates considering both transverse shear and normal deformations.
2. The kinematics of the present theory is much richer than those of the other higher order shear deformation theories, because if the trigonometric term is expanded in power series, the kinematics of higher order theories are implicitly taken into account to a great extent. Moreover, it needs to be noted that every additional power of thickness coordinate in the displacement field of higher-order theories introduces additional unknown variables in those theories which are difficult to interpret physically. Thus, the use of the sinusoidal function in terms of thickness coordinate enhances the richness of the theory and also results in reduction of the number of unknown variables as compared with other competitive displacement-based higher-order theories without loss of the physics of the problem in modeling.
3. In this study, a bending analysis of thick plates resting on Winkler elastic foundation has been carried out. A uniformly distributed layer of Winkler's springs usually represents the elastic foundation. A trigonometric shear and normal deformation theory developed by Ghugal and Sayyad [20-23] is applied for the analytical solutions. The theory has four unknown variables and includes the effect of transverse shear and transverse normal strain. The theory developed is based on certain kinematical and physical assumptions. The governing equations and boundary conditions are obtained using the principle of virtual work. A closed-form solution is obtained using Navier's solution technique. The results obtained for various loading cases are compared with those of the higher order theory of Reddy [3], the first-order shear deformation theory of Mindlin [2], and the classical plate theory [1].
4. The effect of local stress concentration due to concentrated load has assessed effectively by the present theory which has not addressed by the other researchers.

### 2.1. Plate under consideration

Consider a rectangular plate of length ' $a$ ', width ' $b$ ', and total thickness ' $h$ ' made up of linearly elastic isotropic material. The plate occupies a region ( $0 \leq x \leq a$ ,  $0 \leq y \leq b$ ,  $-h/2 \leq z \leq h/2$ ) in Cartesian coordinate system. The plate is resting on Winkler elastic foundation. The geometry and coordinate system of the plate is shown in Fig. 1.

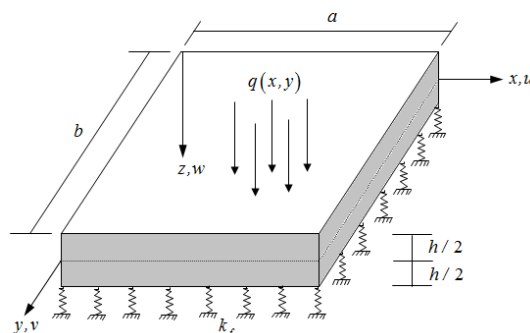


Fig. 1. The geometry and coordinate system of plate

## 2.2. The displacement field, strains and stresses

Based upon the aforementioned assumptions, the displacement field of the present theory is given as below:

$$\begin{aligned} u(x, y, z) &= -z \frac{\partial w(x, y)}{\partial x} + \frac{h}{\pi} \sin \frac{\pi z}{h} \phi(x, y) \\ v(x, y, z) &= -z \frac{\partial w(x, y)}{\partial y} + \frac{h}{\pi} \sin \frac{\pi z}{h} \psi(x, y) \\ w(x, y, z) &= w(x, y) + \frac{h}{\pi} \cos \frac{\pi z}{h} \xi(x, y) \end{aligned} \quad (1)$$

where  $u$ ,  $v$ , and  $w$  are the displacements in  $x$ ,  $y$ , and  $z$  directions, respectively. The trigonometric functions in in-plane displacements are associated with the cosine distribution of transverse shear stress through the thickness of the plate. The  $\phi$ ,  $\psi$  and  $\xi$  are the unknown functions to be determined. The strains associated with the displacement field given by Eq. (1) are obtained within the framework of linear theory of elasticity.

$$\begin{aligned} \varepsilon_x &= \frac{\partial u}{\partial x} = -z \frac{\partial^2 w}{\partial x^2} + \frac{h}{\pi} \sin \frac{\pi z}{h} \frac{\partial \phi}{\partial x} \\ \varepsilon_y &= \frac{\partial v}{\partial y} = -z \frac{\partial^2 w}{\partial y^2} + \frac{h}{\pi} \sin \frac{\pi z}{h} \frac{\partial \psi}{\partial y} \\ \varepsilon_z &= \frac{\partial w}{\partial z} = -\xi \sin \frac{\pi z}{h} \\ \gamma_{xy} &= \frac{\partial u}{\partial x} + \frac{\partial v}{\partial y} = -2z \frac{\partial^2 w}{\partial x \partial y} + \frac{h}{\pi} \sin \frac{\pi z}{h} \left( \frac{\partial \phi}{\partial y} + \frac{\partial \psi}{\partial x} \right) \\ \gamma_{xz} &= \frac{\partial u}{\partial z} + \frac{\partial w}{\partial x} = \cos \frac{\pi z}{h} \left( \frac{h}{\pi} \frac{\partial \xi}{\partial x} + \phi \right) \\ \gamma_{yz} &= \frac{\partial v}{\partial z} + \frac{\partial w}{\partial y} = \cos \frac{\pi z}{h} \left( \frac{h}{\pi} \frac{\partial \xi}{\partial y} + \psi \right) \end{aligned} \quad (2)$$

The three-dimensional stress-strain relationships for the isotropic plate given by Timoshenko and Goodier [15] are used as follows:

$$\begin{aligned} \sigma_x &= \lambda(\varepsilon_x + \varepsilon_y + \varepsilon_z) + 2G\varepsilon_x, \\ \sigma_y &= \lambda(\varepsilon_x + \varepsilon_y + \varepsilon_z) + 2G\varepsilon_y, \\ \sigma_z &= \lambda(\varepsilon_x + \varepsilon_y + \varepsilon_z) + 2G\varepsilon_z, \\ \tau_{xy} &= G\gamma_{xy}, \quad \tau_{xz} = G\gamma_{xz}, \quad \tau_{yz} = G\gamma_{yz} \end{aligned} \quad (3)$$

where  $\lambda$  and  $G$  are the Lamé's constants as given below:

$$\lambda = \frac{\mu E}{(1-\mu)(1-2\mu)} \quad \text{and} \quad G = \frac{E}{2(1+\mu)} \quad (4)$$

The moment and shear force resultants are obtained by integrating stresses through the thickness. The moment resultants ( $M_x$ ,  $M_y$  and  $M_{xy}$ ) analogues to classical plate theory are as follows:

$$\begin{aligned} M_x &= \int_{-h/2}^{h/2} \sigma_x z dz = -L_1 \frac{\partial^2 w}{\partial x^2} - L_2 \frac{\partial^2 w}{\partial y^2} + L_3 \frac{\partial \phi}{\partial x} + L_4 \frac{\partial \psi}{\partial y} - L_5 \xi \\ M_y &= \int_{-h/2}^{h/2} \sigma_y z dz = -L_2 \frac{\partial^2 w}{\partial x^2} - L_1 \frac{\partial^2 w}{\partial y^2} + L_4 \frac{\partial \phi}{\partial x} + L_3 \frac{\partial \psi}{\partial y} - L_5 \xi \\ M_{xy} &= \int_{-h/2}^{h/2} \tau_{xy} z dz = -2L_6 \frac{\partial^2 w}{\partial x \partial y} + L_7 \left( \frac{\partial \psi}{\partial x} + \frac{\partial \phi}{\partial y} \right) \end{aligned} \quad (5)$$

The refined moment resultants ( $M_x^s$ ,  $M_y^s$ ,  $M_z^s$  and  $M_{xy}^s$ ) corresponding to transverse shear deformation are defined as follows:

$$\begin{aligned}
 M_x^s &= \int_{-h/2}^{h/2} \sigma_x \frac{h}{\pi} \sin \frac{\pi z}{h} dz = -L_3 \frac{\partial^2 w}{\partial x^2} - L_4 \frac{\partial^2 w}{\partial y^2} + L_8 \frac{\partial \phi}{\partial x} + L_9 \frac{\partial \psi}{\partial y} - L_{10} \xi \\
 M_y^s &= \int_{-h/2}^{h/2} \sigma_y \frac{h}{\pi} \sin \frac{\pi z}{h} dz = -L_4 \frac{\partial^2 w}{\partial x^2} - L_3 \frac{\partial^2 w}{\partial y^2} + L_9 \frac{\partial \phi}{\partial x} + L_8 \frac{\partial \psi}{\partial y} - L_{10} \xi \\
 M_z^s &= \int_{-h/2}^{h/2} \sigma_z \frac{h}{\pi} \sin \frac{\pi z}{h} dz = -L_5 \left( \frac{\partial^2 w}{\partial x^2} + \frac{\partial^2 w}{\partial y^2} \right) + L_{10} \left( \frac{\partial \phi}{\partial x} + \frac{\partial \psi}{\partial y} \right) - L_{11} \xi \\
 M_{xy}^s &= \int_{-h/2}^{h/2} \tau_{xy} \frac{h}{\pi} \sin \frac{\pi z}{h} dz = -2L_7 \frac{\partial^2 w}{\partial x \partial y} + L_{12} \left( \frac{\partial \psi}{\partial x} + \frac{\partial \phi}{\partial y} \right)
 \end{aligned}
 \tag{6}$$

The shear force resultants ( $Q_x$  and  $Q_y$ ) corresponding to transverse shear deformation are as follows:

$$\begin{aligned}
 Q_x &= \int_{-h/2}^{h/2} \tau_{xz} \cos \frac{\pi z}{h} dz = L_{13} \left( \frac{h}{\pi} \frac{\partial \xi}{\partial x} + \phi \right) \\
 Q_y &= \int_{-h/2}^{h/2} \tau_{yz} \cos \frac{\pi z}{h} dz = L_{13} \left( \frac{h}{\pi} \frac{\partial \xi}{\partial y} + \psi \right)
 \end{aligned}
 \tag{7}$$

and

$$V_x = \frac{\partial M_x}{\partial x} + 2 \frac{\partial M_{xy}}{\partial y} \quad \text{and} \quad V_y = \frac{\partial M_y}{\partial y} + 2 \frac{\partial M_{xy}}{\partial x}
 \tag{8}$$

The constants  $L_1$  to  $L_{12}$  appeared in stress resultants are as follows:

$$\begin{aligned}
 L_1 &= (\lambda + 2G) \frac{h^3}{12}, \quad L_2 = \lambda \frac{h^3}{12}, \quad L_3 = (\lambda + 2G) \frac{2h^3}{\pi^3}, \quad L_4 = \lambda \frac{2h^3}{\pi^3}, \quad L_5 = \lambda \frac{2h^2}{\pi^2}, \quad L_6 = G \frac{h^3}{12}, \\
 L_7 &= G \frac{2h^3}{\pi^3}, \quad L_8 = (\lambda + 2G) \frac{h^3}{2\pi^2}, \quad L_9 = \lambda \frac{h^3}{2\pi^2}, \quad L_{10} = \lambda \frac{h^2}{2\pi}, \quad L_{11} = (\lambda + 2G) \frac{h}{2}, \quad L_{12} = G \frac{h^3}{2\pi^2}, \quad L_{13} = G \frac{h}{2}
 \end{aligned}
 \tag{9}$$

### 2.3. Governing differential equations and boundary conditions for present theory

The governing differential equations and boundary conditions associated with the present theory are obtained using the principle of virtual work given below where  $\delta$  is the variational operator, and  $k_f$  is Winkler modulus.

$$\int_{-h/2}^{h/2} \int_0^b \int_0^a \left[ \sigma_x \delta \varepsilon_x + \sigma_y \delta \varepsilon_y + \sigma_z \delta \varepsilon_z + \tau_{yz} \delta \gamma_{yz} + \tau_{zx} \delta \gamma_{zx} + \tau_{xy} \delta \gamma_{xy} \right] dx dy dz - \int_0^b \int_0^a (q - k_f) \delta w dx dy = 0
 \tag{10}$$

By substituting the strains from Eq. (2) and the stresses from Eq. (3) into Eq. (10), the principle of virtual work can be rewritten as:

$$\begin{aligned}
 &\int_0^b \int_0^a \left( -M_x \frac{\partial^2 \delta w}{\partial x^2} - 2M_{xy} \frac{\partial^2 \delta w}{\partial x \partial y} - M_y \frac{\partial^2 \delta w}{\partial y^2} \right) dx dy + \int_0^b \int_0^a \left( M_x^s \frac{\partial \delta \phi}{\partial x} + M_{xy}^s \frac{\partial \delta \phi}{\partial y} + Q_x \delta \phi \right) dx dy \\
 &+ \int_0^b \int_0^a \left( M_y^s \frac{\partial \delta \psi}{\partial y} + M_{xy}^s \frac{\partial \delta \psi}{\partial x} + Q_y \delta \psi \right) dx dy + \int_0^b \int_0^a \left( Q_x \frac{h}{\pi} \frac{\partial \delta \xi}{\partial x} + Q_y \frac{h}{\pi} \frac{\partial \delta \xi}{\partial y} - M_z^s \delta \xi \right) dx dy = \int_0^b \int_0^a (q - k_f) \delta w dx dy
 \end{aligned}
 \tag{11}$$

By integrating Eq. (11) by parts and collecting coefficients of  $\delta w, \delta \phi, \delta \psi$  and  $\delta \xi$ , one can obtain the following variationally consistent governing equations and associated boundary conditions.

$$\begin{aligned}
 \delta w: & \frac{\partial^2 M_x}{\partial x^2} + 2 \frac{\partial^2 M_{xy}}{\partial x \partial y} + \frac{\partial^2 M_y}{\partial y^2} + q - k_f = 0 \\
 \delta \phi: & \frac{\partial M_x^s}{\partial x} + \frac{\partial M_{xy}^s}{\partial y} - Q_x = 0 \\
 \delta \psi: & \frac{\partial M_y^s}{\partial y} + \frac{\partial M_{xy}^s}{\partial x} - Q_y = 0 \\
 \delta \xi: & \frac{\partial Q_x}{\partial x} + \frac{\partial Q_y}{\partial y} - \frac{\pi}{h} M_z^s = 0
 \end{aligned}
 \tag{12}$$

The boundary conditions obtained at  $x = 0$  and  $x = a$  are of the following form:

$$\begin{aligned}
 &\text{Either } M_x = 0 \quad \text{or } \frac{\partial w}{\partial x} \text{ is prescribed} \\
 &\text{Either } V_x = 0 \quad \text{or } w \text{ is prescribed} \\
 &\text{Either } M_x^s = 0 \quad \text{or } \phi \text{ is prescribed} \\
 &\text{Either } M_{xy}^s = 0 \quad \text{or } \psi \text{ is prescribed} \\
 &\text{Either } Q_x = 0 \quad \text{or } \xi \text{ is prescribed}
 \end{aligned} \tag{13}$$

The boundary conditions obtained at  $y = 0$  and  $y = b$  are of the following form:

$$\begin{aligned}
 &\text{Either } M_y = 0 \quad \text{or } \frac{\partial w}{\partial y} \text{ is prescribed} \\
 &\text{Either } V_y = 0 \quad \text{or } w \text{ is prescribed} \\
 &\text{Either } M_{xy}^s = 0 \quad \text{or } \phi \text{ is prescribed} \\
 &\text{Either } M_y^s = 0 \quad \text{or } \psi \text{ is prescribed} \\
 &\text{Either } Q_y = 0 \quad \text{or } \xi \text{ is prescribed}
 \end{aligned} \tag{14}$$

The governing equations of the plate in terms of displacement variables can be written as follows:

$$D_1 \left( \frac{\partial^4 w}{\partial x^4} + 2 \frac{\partial^4 w}{\partial x^2 \partial y^2} + \frac{\partial^4 w}{\partial y^4} \right) - D_2 \left( \frac{\partial^3 \phi}{\partial x^3} + \frac{\partial^3 \phi}{\partial x \partial y^2} + \frac{\partial^3 \psi}{\partial y^3} + \frac{\partial^3 \psi}{\partial x^2 \partial y} \right) + D_3 \left( \frac{\partial^2 \xi}{\partial x^2} + \frac{\partial^2 \xi}{\partial y^2} \right) = q - k_f \tag{15}$$

$$D_2 \left( \frac{\partial^3 w}{\partial x^3} + \frac{\partial^3 w}{\partial x \partial y^2} \right) - \left( D_4 \frac{\partial^2 \phi}{\partial x^2} + D_5 \frac{\partial^2 \phi}{\partial y^2} - D_6 \phi \right) + D_7 \frac{\partial^2 \psi}{\partial x \partial y} + D_8 \frac{\partial \xi}{\partial x} = 0 \tag{16}$$

$$D_2 \left( \frac{\partial^3 w}{\partial y^3} + \frac{\partial^3 w}{\partial x^2 \partial y} \right) + D_7 \frac{\partial^2 \phi}{\partial x \partial y} - \left( D_4 \frac{\partial^2 \psi}{\partial y^2} + D_5 \frac{\partial^2 \psi}{\partial x^2} - D_6 \psi \right) + D_8 \frac{\partial \xi}{\partial y} = 0 \tag{17}$$

$$D_3 \left( \frac{\partial^2 w}{\partial y^2} + \frac{\partial^2 w}{\partial x^2} \right) - D_8 \left( \frac{\partial \phi}{\partial x} + \frac{\partial \psi}{\partial y} \right) - D_5 \left( \frac{\partial^2 \xi}{\partial x^2} + \frac{\partial^2 \xi}{\partial y^2} \right) - D_9 \xi = 0 \tag{18}$$

where  $D_1$  through  $D_9$  are the stiffnesses as given below:

$$\begin{aligned}
 D_1 &= (\lambda + 2G) \frac{h^3}{12}, \quad D_2 = (\lambda + 2G) \frac{2h^3}{\pi^3}, \quad D_3 = \lambda \frac{2h^2}{\pi^2}, \quad D_4 = (\lambda + 2G) \frac{h^3}{2\pi^2}, \\
 D_5 &= G \frac{h^3}{2\pi^2}, \quad D_6 = G \frac{h}{2}, \quad D_7 = (\lambda + G) \frac{h^3}{2\pi^2}, \quad D_8 = (\lambda + G) \frac{h^2}{2\pi}, \quad D_9 = (\lambda + G) \frac{h}{2}
 \end{aligned} \tag{19}$$

### 3. Analytical solution using double trigonometric series (The Navier solution)

To prove the efficiency and validity of the presented theory, the bending analysis of a simply supported plate resting on Winkler elastic foundation is considered. The plate is subjected to a transverse load,  $q(x, y)$  on the top surface of the plate (i.e.  $z = -h/2$ ). Six different types of static loading conditions are considered for the detailed numerical study. Navier's solution technique is employed to determine numerical solution for the simply supported plate. The following are the boundary conditions of the simply supported plate.

At edges  $x = 0, x = a$ :

$$w = \psi = \xi = M_x = M_x^s = 0 \tag{20}$$

At edges  $y = 0, y = b$ :

$$w = \phi = \xi = M_y = M_y^s = 0 \tag{21}$$

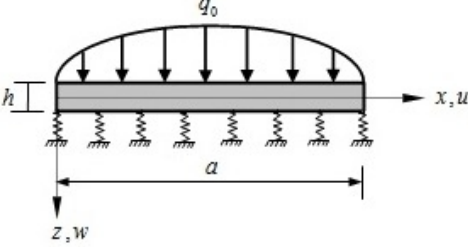
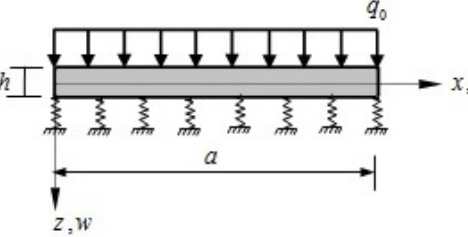
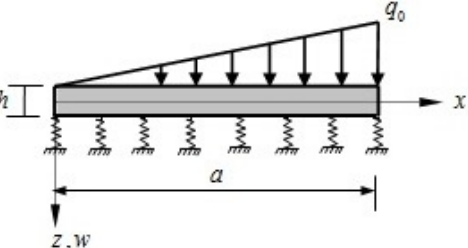
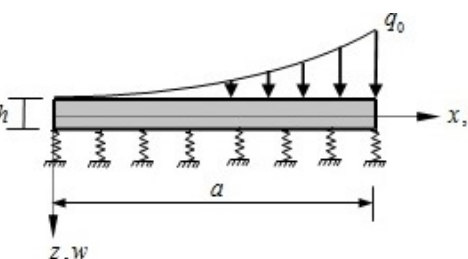
According to Navier solution technique, the transverse load can be expressed in double trigonometric series as:

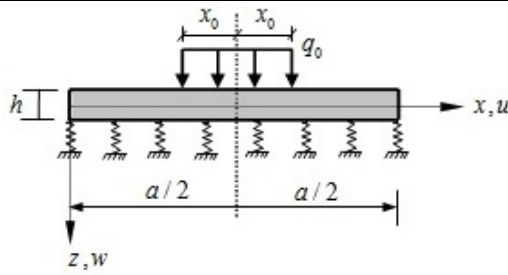
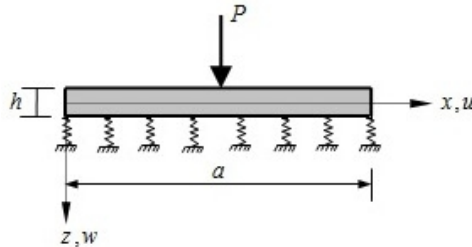
$$q(x, y) = \sum_{m=1,3,5}^{\infty} \sum_{n=1,3,5}^{\infty} q_{mn} \sin\left(\frac{m\pi x}{a}\right) \sin\left(\frac{n\pi y}{b}\right) \tag{22}$$

where  $q_{mn}$  is the coefficient of Fourier expansion of load. The values of this coefficient for various loading cases are obtained using Eq. (23) and are given in Table 1.

$$q_{mn} = \frac{4}{ab} \int_0^b \int_0^a q(x,y) \sin \frac{m\pi x}{a} \sin \frac{n\pi y}{b} dx dy \tag{23}$$

**Table 1.** Coefficients ( $q_{mn}$ ) in the double trigonometric series expansion of loads in the Navier method

Load	$q_{mn}$
<p>Sinusoidally distributed load <math>q(x,y) = q_0</math></p> 	$q_{mn} = q_0$ $(m = 1, n = 1)$
<p>Uniformly distributed load <math>q(x,y) = q_0</math></p> 	$q_{mn} = \frac{16q_0}{mn\pi^2}$ $(m = 25, n = 25)$
<p>Linearly varying or hydrostatic load</p> $q(x,y) = \frac{q_0 x}{a}$ 	$q_{mn} = \frac{8q_0}{mn\pi^2} \cos m\pi$ $(m = 25, n = 25)$
<p>Parabolic load <math>q(x,y) = q_0 \left(\frac{x}{a}\right)^2</math></p> 	$q_{mn} = \frac{4q_0}{mn\pi^2} I, \quad (m = 25, n = 25)$ $I = \left[ \begin{matrix} \frac{2}{m\pi} \sin m\pi + \frac{2}{m^2\pi^2} \cos m\pi \\ -\cos m\pi - \frac{2}{m^2\pi^2} \end{matrix} \right] (1 - \cos n\pi)$
<p>Central patch load <math>q(x,y) = q_0</math></p>	$q_{mn} = \frac{16q_0}{mn\pi^2} \sin \frac{m\pi x_0}{2} \sin \frac{n\pi y_0}{2}$ $(m = 25, n = 25, x_0 = 0.02a, y_0 = 0.02b)$


 Central concentrated load  $q(x,y) = P$ 


$$q_{mn} = \frac{4P}{ab} \sin \frac{m\pi}{2} \sin \frac{n\pi}{2}$$

$$(m = 25, n = 25)$$

The following is the solution form assumed for unknown variables in the displacement field which exactly satisfies simply supported boundary conditions:

$$\begin{aligned} w(x,y) &= \sum_{m=1,3,5}^{\infty} \sum_{n=1,3,5}^{\infty} w_{mn} \sin \frac{m\pi x}{a} \sin \frac{n\pi y}{b} \\ \phi(x,y) &= \sum_{m=1,3,5}^{\infty} \sum_{n=1,3,5}^{\infty} \phi_{mn} \cos \frac{m\pi x}{a} \sin \frac{n\pi y}{b} \\ \psi(x,y) &= \sum_{m=1,3,5}^{\infty} \sum_{n=1,3,5}^{\infty} \psi_{mn} \sin \frac{m\pi x}{a} \cos \frac{n\pi y}{b} \\ \xi(x,y) &= \sum_{m=1,3,5}^{\infty} \sum_{n=1,3,5}^{\infty} \xi_{mn} \sin \frac{m\pi x}{a} \sin \frac{n\pi y}{b} \end{aligned} \quad (24)$$

where  $w_{mn}$ ,  $\phi_{mn}$ ,  $\psi_{mn}$  and  $\xi_{mn}$  are the unknown coefficients of the respective Fourier expansions and  $m, n$  are positive integers. Substitution of the load  $q(x,y)$  from Eq. (22) and solution form from Eq. (24) into the Eqs. (15) - (18) yields the four algebraic simultaneous equations in the following matrix form.

$$\begin{bmatrix} K_{11} & K_{12} & K_{13} & K_{14} \\ K_{21} & K_{22} & K_{23} & K_{24} \\ K_{31} & K_{32} & K_{33} & K_{34} \\ K_{41} & K_{42} & K_{43} & K_{44} \end{bmatrix} \begin{Bmatrix} w_{mn} \\ \phi_{mn} \\ \psi_{mn} \\ \xi_{mn} \end{Bmatrix} = \begin{Bmatrix} q_{mn} \\ 0 \\ 0 \\ 0 \end{Bmatrix} \quad (25)$$

where elements of stiffness matrix  $[K]$  are as follows:

$$\begin{aligned} K_{11} &= D_1 \left( \frac{m^4 \pi^4}{a^4} + 2 \frac{m^2 n^2 \pi^4}{a^2 b^2} + \frac{n^4 \pi^4}{b^4} \right) + k_f, & K_{12} &= -D_2 \left( \frac{m^3 \pi^3}{a^3} + \frac{m n^2 \pi^3}{a b^2} \right), & K_{13} &= -D_2 \left( \frac{n^3 \pi^3}{b^3} + \frac{n m^2 \pi^3}{b a^2} \right), \\ K_{14} &= -D_3 \left( \frac{m^2 \pi^2}{a^2} + \frac{n^2 \pi^2}{b^2} \right), & K_{22} &= D_4 \frac{m^2 \pi^2}{a^2} + D_5 \frac{n^2 \pi^2}{b^2} + D_6, & K_{23} &= -D_7 \frac{m n \pi^2}{a b}, & K_{24} &= D_8 \frac{m \pi}{a}, \\ K_{33} &= D_4 \frac{n^2 \pi^2}{b^2} + D_5 \frac{m^2 \pi^2}{a^2} + D_6, & K_{34} &= D_8 \frac{n \pi}{b}, & K_{44} &= D_5 \left( \frac{m^2 \pi^2}{a^2} + \frac{n^2 \pi^2}{b^2} \right) - D_9. \end{aligned} \quad (26)$$

Solving Eq. (25) gives the values of  $w_{mn}$ ,  $\phi_{mn}$ ,  $\psi_{mn}$  and  $\xi_{mn}$ . Having these values, one can then calculate all the displacement and stress components within the plate using Eqs. (1) - (3). Transverse shear stresses can be obtained by either constitutive relations or integrating equilibrium equations of the theory of elasticity. These stresses are indicated by  $\tau_{xz}^{CR}$  and  $\tau_{yz}^{CR}$  when obtained by constitutive relations and are indicated by  $\tau_{xz}^{EE}$  and  $\tau_{yz}^{EE}$  when obtained by using equilibrium equations. The equilibrium equations of the theory of elasticity are given below.

$$\frac{\partial \sigma_x}{\partial x} + \frac{\partial \tau_{xy}}{\partial y} + \frac{\partial \tau_{xz}}{\partial z} = 0, \quad \frac{\partial \sigma_y}{\partial y} + \frac{\partial \tau_{xy}}{\partial x} + \frac{\partial \tau_{yz}}{\partial z} = 0, \quad \frac{\partial \tau_{xz}}{\partial x} + \frac{\partial \tau_{yz}}{\partial y} + \frac{\partial \sigma_z}{\partial z} = 0 \tag{27}$$

### 4. Numerical results and discussion

The numerical results are obtained for isotropic square ( $b = a$ ) plates subjected to different static loadings. The following material properties are used for the plate.

$$E = 210 \text{ GPa}, \quad \mu = 0.3 \quad \text{and} \quad G = \frac{E}{2(1 + \mu)} \tag{28}$$

where ‘ $E$ ’ is Young’s modulus, ‘ $\mu$ ’ is Poisson’s ratio, and ‘ $G$ ’ is Shear modulus. The transverse deflection ( $w$ ), in-plane stresses ( $\sigma_x, \sigma_y, \tau_{xy}$ ), and transverse shear stresses ( $\tau_{xz}, \tau_{yz}$ ) are presented in the following normalized form for the purpose of presenting the results.

$$K^4 = \frac{k_f a^4}{D}, \quad \bar{w}\left(\frac{a}{2}, \frac{b}{2}, 0\right) = \frac{100 E w}{q_0 h S^4}, \quad (\bar{\sigma}_x, \bar{\sigma}_y)\left(0, 0, \pm \frac{h}{2}\right) = \frac{(\sigma_x, \sigma_y)}{q_0 S^2}, \tag{29}$$

$$\bar{\tau}_{xy}\left(\frac{a}{2}, \frac{b}{2}, \pm \frac{h}{2}\right) = \frac{\tau_{xy}}{q_0 S^2}, \quad \bar{\tau}_{zx}\left(\frac{a}{2}, 0, 0\right) = \frac{\tau_{zx}}{q_0 S}, \quad \bar{\tau}_{yz}\left(0, \frac{b}{2}, 0\right) = \frac{\tau_{yz}}{q_0 S}$$

Here,  $S$  is the aspect ratio ( $a/h$ ) of the plate. In case of central point load  $q_0$  becomes  $P$ . Since an exact three-dimensional elasticity solution for bending of the isotropic plate resting on Winkler elastic foundation is not available in the literature, the present results are compared and discussed with the corresponding results of the classical plate theory (CPT), first-order shear deformation theory (FSDT), and higher order shear deformation theory of Reddy (HSDT). The numerical results are obtained for different values of foundation modulus ( $K = 1, 3, 5$ ) and aspect ratios ( $S = 4, 10, 100$ ).

#### 4.1. A simply supported isotropic plate subjected to sinusoidally distributed load

The normalized transverse displacement and stresses for the isotropic square plate subjected to sinusoidally distributed load are shown in Table 2. The examination of this table reveals that the results of displacement and stresses obtained by the present theory are in good agreement with those of Reddy’s theory. CPT underestimates the value of transverse displacement for aspect ratios 4 and 10. The in-plane stresses predicted by FSDT and CPT are closer to each other.

#### 4.2. A simply supported isotropic plate subjected to uniformly distributed load

Table 3 shows the comparison of transverse displacement and stresses for the isotropic square plate subjected to uniformly distributed load. The through-thickness distributions of in-plane normal stress and transverse shear stress for different foundation modulus are plotted in Figs. 2 and 3, respectively. Table 3 shows that the transverse displacement and stresses obtained by using the present theory are in excellent agreement with those of Reddy’s theory. It is also observed that the transverse displacements and in-plane stresses are decreased with an increase in aspect ratio as well as foundation modulus. The numerical results obtained by all the theories are more or less the same for the thin plate ( $S = 100$ ).

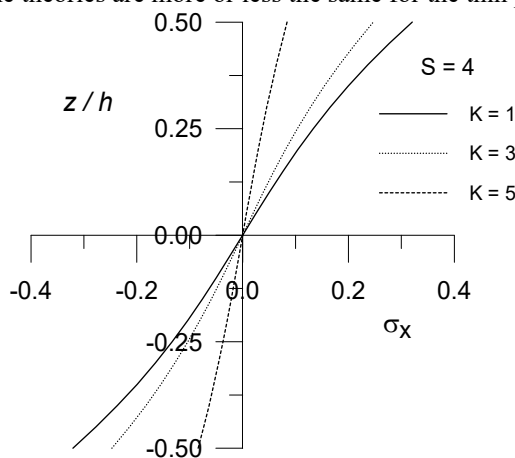


Fig. 2. Through thickness distribution of in-plane normal stress ( $\bar{\sigma}_x$ ) for isotropic square plate subjected to uniformly distributed load



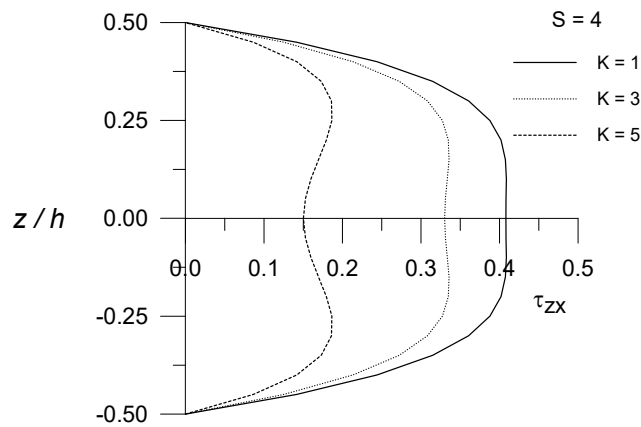


Fig. 3. Through thickness distribution of transverse shear stress ( $\bar{\tau}_{zx}^{EE}$ ) for isotropic square plate subjected to uniformly distributed load

**4.3. A simply supported isotropic plate subjected to linearly varying (Hydrostatic) load**

The comparison of transverse displacement and stresses for the isotropic square plate subjected to a linearly (Hydrostatic) load is reported in Table 4. The intensity of load ( $q_0$ ) is zero at edge  $x = 0$  and maximum at  $x = a$ . From Table 4 it is figured out that the present theory predicts the transverse displacement and stresses very accurately compared with those of Reddy’s theory. FSDT and CPT show more or less the same values for stresses.

**4.4. A simply supported isotropic plate subjected to parabolic load**

In this example, bending analysis of the isotropic square plate is carried out for a parabolic load. The intensity of load ( $q_0$ ) is zero at edge  $x = 0$  and maximum at edge  $x = a$ . The numerical results are reported in Table 5 and found to agree well with those of Reddy’s theory. FSDT and CPT underestimate the values of transverse displacement and in-plane stresses, whereas they overestimate the values of transverse shear stresses.

**4.5. A simply supported isotropic plate subjected to central patch load**

In this example, bending response of the isotropic square plate is examined under the patch load. The load is centrally applied with size  $x_0 \times y_0$ . The value of  $x_0=0.02a$  and  $y_0=0.02b$ . The transverse displacement and stresses for various aspect ratios and foundation moduli are reported in Table 6. The examination of Table 6 reveals that as compared with other loading cases discussed in the preceding sections, the stresses developed due to central patch load are very small. It is also seen that the present results are in excellent agreement with those of Reddy’s theory.

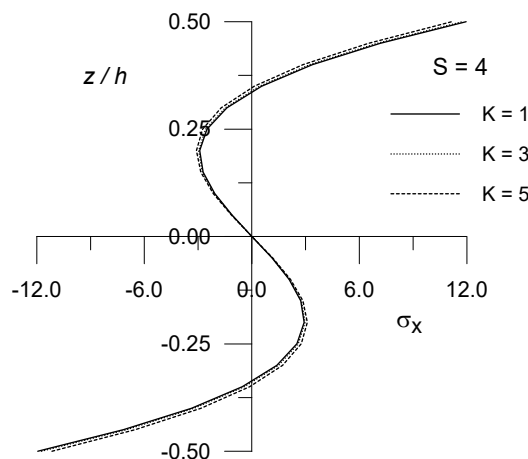


Fig. 4. Through thickness distribution of in-plane normal stress ( $\bar{\sigma}_x$ ) for isotropic square plate subjected to central concentrated load

**4.6. A simply supported isotropic plate subjected to central concentrated load**

The displacements and stresses for the isotropic square plate when subjected to a central concentrated load are shown in Table 7. The through-thickness distributions of in-plane normal stress are shown in Fig. 4 for  $S = 4$  and  $K = 1, 3, 5$ . The variation of this stress is non-linear through the thickness, which may be the effect of local stress concentration due to concentrated load,

that cannot be captured by the classical theories. The through-thickness distributions of transverse shear stress ( $\bar{\tau}_{zx}^{EE}$ ) when obtained by using equation of equilibrium is shown in Fig. 5. These distributions are plotted for the aspect ratio 4 and foundation modulus 1, 3, and 5. The distributions show that the maximum transverse shear stress occurs at  $z = \pm 0.35 h$  instead of at neutral plane. However, these distributions show the negative values at neutral plane. This anomalous behavior of transverse shear stress may be attributed to the effect of local stress concentration due to concentrated load.

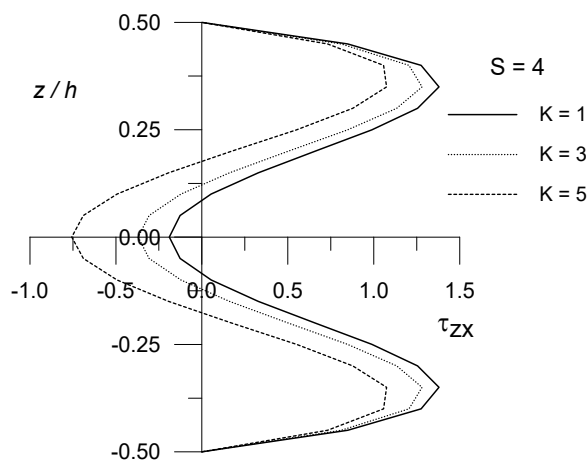


Fig. 5. Through thickness distribution of transverse shear stress ( $\bar{\tau}_{zx}^{EE}$ ) for isotropic square plate subjected to central concentrated load

Table 2. Comparison of non-dimensional deflection and stresses in isotropic square plate subjected to sinusoidally distributed load

S	K	Theory	$\bar{w}$	$\bar{\sigma}_x$	$\bar{\sigma}_y$	$\bar{\tau}_{xy}$	$\bar{\tau}_{zx}^{CR}$	$\bar{\tau}_{zx}^{EE}$	$\bar{\tau}_{yz}^{CR}$	$\bar{\tau}_{yz}^{EE}$
4	1	Present	3.3348	0.2260	0.2260	0.1060	0.2437	0.2319	0.2437	0.2319
		HSDT [3]	3.4554	0.2084	0.2084	0.1122	0.2369	0.2344	0.2369	0.2344
		FSDT [2]	3.3094	0.1969	0.1969	0.1060	0.1586	0.2379	0.1586	0.2379
		CPT [1]	2.5599	0.1971	0.1971	0.1061	---	0.2381	---	0.2381
	3	Present	2.6531	0.1798	0.1798	0.0843	0.1938	0.1845	0.1938	0.1845
		HSDT [3]	2.7071	0.1633	0.1633	0.0879	0.1856	0.1837	0.1856	0.1837
		FSDT [2]	2.6166	0.1557	0.1557	0.0838	0.1254	0.1881	0.1254	0.1881
		CPT [1]	2.1248	0.1636	0.1636	0.0881	---	0.1976	---	0.1976
	5	Present	1.1100	0.0752	0.0752	0.0353	0.0811	0.0772	0.0811	0.0772
		HSDT [3]	1.0948	0.0660	0.0660	0.0356	0.0751	0.0743	0.0751	0.0743
		FSDT [2]	1.0797	0.0642	0.0642	0.0346	0.0518	0.0776	0.0518	0.0776
		CPT [1]	0.9856	0.0759	0.0759	0.0409	---	0.0917	---	0.0917
10	1	Present	2.6791	0.2119	0.2119	0.1059	0.2448	0.2351	0.2448	0.2351
		HSDT [3]	2.7038	0.1989	0.1989	0.1071	0.2379	0.2375	0.2379	0.2375
		FSDT [2]	2.6799	0.1970	0.1970	0.1061	0.1587	0.2381	0.1587	0.2381
		CPT [1]	2.5599	0.1971	0.1971	0.1061	---	0.2381	---	0.2381
	3	Present	2.2101	0.1748	0.1748	0.0872	0.2019	0.1939	0.2019	0.1939
		HSDT [3]	2.2230	0.1635	0.1635	0.0881	0.1956	0.1953	0.1956	0.1953
		FSDT [2]	2.2068	0.1623	0.1623	0.0874	0.1307	0.1961	0.1307	0.1961
		CPT [1]	2.1248	0.1636	0.1636	0.0881	---	0.1976	---	0.1976
	5	Present	1.0090	0.0798	0.0798	0.0398	0.0922	0.0885	0.0922	0.0885
		HSDT [3]	1.0062	0.0740	0.0740	0.0399	0.0885	0.0884	0.0885	0.0884
		FSDT [2]	1.0029	0.0737	0.0737	0.0397	0.0594	0.0891	0.0594	0.0891
		CPT [1]	0.9856	0.0759	0.0759	0.0409	---	0.0917	---	0.0917
100	1	Present	2.5529	0.2093	0.2093	0.1058	0.2450	0.2356	0.2450	0.2356
		HSDT [3]	2.5619	0.1971	0.1971	0.1061	0.2381	0.2382	0.2381	0.2382
		FSDT [2]	2.5603	0.1970	0.1970	0.1061	0.1587	0.2380	0.1587	0.2380
		CPT [1]	2.5599	0.1971	0.1971	0.1061	---	0.2381	---	0.2381
	3	Present	2.1200	0.1738	0.1738	0.0878	0.2034	0.1957	0.2034	0.1957
		HSDT [3]	2.1262	0.1636	0.1636	0.0881	0.1976	0.1977	0.1976	0.1977
		FSDT [2]	2.1251	0.1635	0.1635	0.0880	0.1317	0.1976	0.1317	0.1976
		CPT [1]	2.1248	0.1636	0.1636	0.0881	---	0.1976	---	0.1976
	5	Present	0.9846	0.0807	0.0807	0.0408	0.0945	0.0909	0.0945	0.0909
		HSDT [3]	0.9859	0.0759	0.0759	0.0408	0.0916	0.0917	0.0916	0.0917

FSDT [2]	0.9856	0.0758	0.0758	0.0408	0.0611	0.0916	0.0611	0.0916
CPT [1]	0.9856	0.0759	0.0759	0.0409	---	0.0917	---	0.0917

**Table 3.** Comparison of non-dimensional deflection and stresses in isotropic square plate subjected to uniformly distributed load

<i>S</i>	<i>K</i>	Theory	$\bar{w}$	$\bar{\sigma}_x$	$\bar{\sigma}_y$	$\bar{\tau}_{xy}$	$\bar{\tau}_{xz}^{CR}$	$\bar{\tau}_{zx}^{EE}$	$\bar{\tau}_{yz}^{CR}$	$\bar{\tau}_{zy}^{EE}$
4	1	Present	5.1840	0.3206	0.3206	0.2076	0.4820	0.4087	0.4820	0.4087
		HSDT [3]	5.3548	0.2980	0.2980	0.2174	0.4814	0.4507	0.4814	0.4507
		FSDT [2]	5.1410	0.2863	0.2863	0.1942	0.3292	0.4937	0.3292	0.4937
		CPT [1]	4.0517	0.2865	0.2865	0.1943	---	0.4940	---	0.4940
	3	Present	4.0838	0.2469	0.2469	0.1721	0.4001	0.3356	0.4001	0.3356
		HSDT [3]	4.1478	0.2259	0.2259	0.1775	0.3970	0.3672	0.3970	0.3672
		FSDT [2]	4.0230	0.2202	0.2202	0.1579	0.2746	0.4118	0.2746	0.4118
		CPT [1]	3.3472	0.2326	0.2326	0.1649	---	0.4280	---	0.4280
	5	Present	1.6117	0.0841	0.0841	0.0904	0.2101	0.1864	0.2101	0.1864
		HSDT [3]	1.5693	0.0744	0.0744	0.0897	0.2106	0.1833	0.2106	0.1833
		FSDT [2]	1.5609	0.0765	0.0765	0.0761	0.1506	0.2259	0.1506	0.2259
		CPT [1]	1.5060	0.0924	0.0924	0.0876	---	0.2534	---	0.2534
10	1	Present	4.2240	0.3071	0.3071	0.1950	0.5033	0.4811	0.5033	0.4811
		HSDT [3]	4.2609	0.2884	0.2884	0.2028	0.4914	0.4851	0.4914	0.4851
		FSDT [2]	4.2261	0.2865	0.2865	0.1943	0.3293	0.4940	0.3293	0.4940
		CPT [1]	4.0517	0.2865	0.2865	0.1943	---	0.4940	---	0.4940
	3	Present	3.4650	0.2474	0.2474	0.1648	0.4333	0.4066	0.4333	0.4066
		HSDT [3]	3.4828	0.2315	0.2315	0.1718	0.4223	0.4161	0.4223	0.4161
		FSDT [2]	3.4605	0.2305	0.2305	0.1637	0.2835	0.4253	0.2835	0.4253
		CPT [1]	3.3472	0.2326	0.2326	0.1649	---	0.4280	---	0.4280
	5	Present	1.5260	0.0961	0.0961	0.0870	0.2520	0.2324	0.2520	0.2324
		HSDT [3]	1.5191	0.0891	0.0891	0.0924	0.2451	0.2393	0.2451	0.2393
		FSDT [2]	1.5170	0.0895	0.0895	0.0855	0.1656	0.2484	0.1656	0.2484
		CPT [1]	1.5060	0.0924	0.0924	0.0876	---	0.2534	---	0.2534
100	1	Present	4.0405	0.3044	0.3044	0.1937	0.5082	0.4941	0.5082	0.4941
		HSDT [3]	4.0547	0.2866	0.2866	0.1999	0.4940	0.4940	0.4940	0.4940
		FSDT [2]	4.0521	0.2864	0.2864	0.1942	0.3293	0.4939	0.3293	0.4939
		CPT [1]	4.0517	0.2865	0.2865	0.1943	---	0.4940	---	0.4940
	3	Present	3.3395	0.2472	0.2472	0.1645	0.4404	0.4236	0.4404	0.4236
		HSDT [3]	3.3492	0.2326	0.2326	0.1705	0.4279	0.4279	0.4279	0.4279
		FSDT [2]	3.3475	0.2325	0.2325	0.1649	0.2852	0.4279	0.2852	0.4279
		CPT [1]	3.3472	0.2326	0.2326	0.1649	---	0.4280	---	0.4280
	5	Present	1.5045	0.0984	0.0984	0.0874	0.2610	0.2510	0.2610	0.2510
		HSDT [3]	1.5062	0.0924	0.0924	0.0930	0.2533	0.2533	0.2533	0.2533
		FSDT [2]	1.5059	0.0924	0.0924	0.0876	0.1689	0.2534	0.1689	0.2534
		CPT [1]	1.5060	0.0924	0.0924	0.0876	---	0.2534	---	0.2534

**Table 4.** Comparison of non-dimensional deflection and stresses in isotropic square plate subjected to linearly varying (Hydrostatic) load

<i>S</i>	<i>K</i>	Theory	$\bar{w}$	$\bar{\sigma}_x$	$\bar{\sigma}_y$	$\bar{\tau}_{xy}$	$\bar{\tau}_{xz}^{CR}$	$\bar{\tau}_{zx}^{EE}$	$\bar{\tau}_{yz}^{CR}$	$\bar{\tau}_{zy}^{EE}$
4	1	Present	2.5920	0.1603	0.1603	0.1038	0.2410	0.2044	0.2410	0.2044
		HSDT [3]	2.6774	0.1490	0.1490	0.1087	0.2407	0.2254	0.2407	0.2254
		FSDT [2]	2.5705	0.1432	0.1432	0.0971	0.1646	0.2469	0.1646	0.2469
		CPT [1]	2.0259	0.1433	0.1433	0.0972	---	0.2470	---	0.2470
	3	Present	2.0419	0.1235	0.1235	0.0861	0.2001	0.1678	0.2001	0.1678
		HSDT [3]	2.0739	0.1130	0.1130	0.0888	0.1985	0.1836	0.1985	0.1836
		FSDT [2]	2.0115	0.1101	0.1101	0.0790	0.1373	0.2059	0.1373	0.2059
		CPT [1]	1.6736	0.1163	0.1163	0.0825	---	0.2140	---	0.2140
	5	Present	0.8059	0.0421	0.0421	0.0452	0.1051	0.0932	0.1051	0.0932
		HSDT [3]	0.7847	0.0372	0.0372	0.0449	0.1053	0.0917	0.1053	0.0917
		FSDT [2]	0.7805	0.0383	0.0383	0.0381	0.0753	0.1130	0.0753	0.1130
		CPT [1]	0.7530	0.0462	0.0462	0.0438	---	0.1267	---	0.1267
10	1	Present	2.1120	0.1536	0.1536	0.0975	0.2517	0.2406	0.2517	0.2406
	HSDT [3]	2.1305	0.1442	0.1442	0.1014	0.2457	0.2426	0.2457	0.2426	

		FSDT [2]	2.1131	0.1433	0.1433	0.0972	0.1647	0.2470	0.1647	0.2470
		CPT [1]	2.0259	0.1433	0.1433	0.0972	---	0.2470	---	0.2470
3		Present	1.7325	0.1237	0.1237	0.0824	0.2167	0.2033	0.2167	0.2033
		HSDT [3]	1.7414	0.1158	0.1158	0.0859	0.2112	0.2081	0.2112	0.2081
		FSDT [2]	1.7303	0.1153	0.1153	0.0819	0.1418	0.2127	0.1418	0.2127
		CPT [1]	1.6736	0.1163	0.1163	0.0825	---	0.2140	---	0.2140
5		Present	0.7630	0.0481	0.0481	0.0435	0.1260	0.1162	0.1260	0.1162
		HSDT [3]	0.7596	0.0446	0.0446	0.0462	0.1226	0.1197	0.1226	0.1197
		FSDT [2]	0.7585	0.0448	0.0448	0.0428	0.0828	0.1242	0.0828	0.1242
		CPT [1]	0.7530	0.0462	0.0462	0.0438	---	0.1267	---	0.1267
100	1	Present	2.0203	0.1522	0.1522	0.0969	0.2541	0.2471	0.2541	0.2471
		HSDT [3]	2.0274	0.1433	0.1433	0.1000	0.2470	0.2470	0.2470	0.2470
		FSDT [2]	2.0261	0.1432	0.1432	0.0971	0.1647	0.2470	0.1647	0.2470
		CPT [1]	2.0259	0.1433	0.1433	0.0972	---	0.2470	---	0.2470
	3	Present	1.6698	0.1236	0.1236	0.0823	0.2202	0.2118	0.2202	0.2118
		HSDT [3]	1.6746	0.1163	0.1163	0.0853	0.2140	0.2140	0.2140	0.2140
		FSDT [2]	1.6738	0.1163	0.1163	0.0825	0.1426	0.2140	0.1426	0.2140
		CPT [1]	1.6736	0.1163	0.1163	0.0825	---	0.2140	---	0.2140
	5	Present	0.7523	0.0492	0.0492	0.0437	0.1305	0.1255	0.1305	0.1255
		HSDT [3]	0.7531	0.0462	0.0462	0.0465	0.1267	0.1267	0.1267	0.1267
		FSDT [2]	0.7530	0.0462	0.0462	0.0438	0.0845	0.1267	0.0845	0.1267
		CPT [1]	0.7530	0.0462	0.0462	0.0438	---	0.1267	---	0.1267

**Table 5.** Comparison of non-dimensional deflection and stresses in isotropic square plate subjected to parabolic load

$S$	$K$	Theory	$\bar{w}$	$\bar{\sigma}_x$	$\bar{\sigma}_y$	$\bar{\tau}_{xy}$	$\bar{\tau}_{zx}^{CR}$	$\bar{\tau}_{zx}^{EE}$	$\bar{\tau}_{yz}^{CR}$	$\bar{\tau}_{yz}^{EE}$
4	1	Present	1.5228	0.0903	0.0903	0.0666	0.1636	0.1303	0.1636	0.1303
		HSDT [3]	1.5716	0.0838	0.0838	0.0691	0.1654	0.1508	0.1654	0.1508
		FSDT [2]	1.5100	0.0811	0.0811	0.0603	0.1142	0.1712	0.1142	0.1712
		CPT [1]	1.1964	0.0812	0.0812	0.0603	---	0.1713	---	0.1713
	3	Present	1.1961	0.0685	0.0685	0.0560	0.1389	0.1069	0.1389	0.1069
		HSDT [3]	1.2133	0.0625	0.0625	0.0571	0.1400	0.1257	0.1400	0.1257
		FSDT [2]	1.1780	0.0616	0.0616	0.0495	0.0977	0.1466	0.0977	0.1466
		CPT [1]	0.9870	0.0652	0.0652	0.0516	---	0.1516	---	0.1516
	5	Present	0.4636	0.0209	0.0209	0.0314	0.0806	0.0519	0.0806	0.0519
		HSDT [3]	0.4496	0.0182	0.0182	0.0307	0.0827	0.0693	0.0827	0.0693
		FSDT [2]	0.4484	0.0194	0.0194	0.0250	0.0597	0.0895	0.0597	0.0895
		CPT [1]	0.4400	0.0238	0.0238	0.0285	---	0.0989	---	0.0989
10	1	Present	1.2459	0.0870	0.0870	0.0608	0.1739	0.1622	0.1739	0.1622
		HSDT [3]	1.2566	0.0816	0.0816	0.0644	0.1701	0.1671	0.1701	0.1671
		FSDT [2]	1.2466	0.0812	0.0812	0.0603	0.1142	0.1713	0.1142	0.1713
		CPT [1]	1.1964	0.0812	0.0812	0.0603	---	0.1713	---	0.1713
	3	Present	1.0203	0.0693	0.0693	0.0518	0.1529	0.1421	0.1529	0.1421
		HSDT [3]	1.0254	0.0648	0.0648	0.0551	0.1494	0.1464	0.1494	0.1464
		FSDT [2]	1.0190	0.0646	0.0646	0.0512	0.1005	0.1508	0.1005	0.1508
		CPT [1]	0.9870	0.0652	0.0652	0.0516	---	0.1516	---	0.1516
	5	Present	0.4445	0.0247	0.0247	0.0286	0.0981	0.0894	0.0981	0.0894
		HSDT [3]	0.4422	0.0227	0.0227	0.0313	0.0958	0.0929	0.0958	0.0929
		FSDT [2]	0.4419	0.0230	0.0230	0.0279	0.0648	0.0972	0.0648	0.0972
		CPT [1]	0.4400	0.0238	0.0238	0.0285	---	0.0989	---	0.0989
100	1	Present	1.1931	0.0863	0.0863	0.0601	0.1762	0.1695	0.1762	0.1695
		HSDT [3]	1.1973	0.0812	0.0812	0.0634	0.1713	0.1713	0.1713	0.1713
		FSDT [2]	1.1965	0.0812	0.0812	0.0603	0.1142	0.1713	0.1142	0.1713
		CPT [1]	1.1964	0.0812	0.0812	0.0603	---	0.1713	---	0.1713
	3	Present	0.9847	0.0694	0.0694	0.0514	0.1560	0.1500	0.1560	0.1500
		HSDT [3]	0.9876	0.0652	0.0652	0.0547	0.1516	0.1515	0.1516	0.1515
		FSDT [2]	0.9870	0.0651	0.0651	0.0516	0.1010	0.1515	0.1010	0.1515
		CPT [1]	0.9870	0.0652	0.0652	0.0516	---	0.1516	---	0.1516
	5	Present	0.4395	0.0254	0.0254	0.0285	0.1018	0.0979	0.1018	0.0979
		HSDT [3]	0.4400	0.0238	0.0238	0.0315	0.0989	0.0989	0.0989	0.0989

FSDT [2]	0.4399	0.0238	0.0238	0.0285	0.0659	0.0989	0.0659	0.0989
CPT [1]	0.4400	0.0238	0.0238	0.0285	---	0.0989	---	0.0989

**Table 6.** Comparison of non-dimensional deflection and stresses in isotropic square plate subjected to central patch load

<i>S</i>	<i>K</i>	Theory	$\bar{w}$	$\bar{\sigma}_x$	$\bar{\sigma}_y$	$\bar{\tau}_{xy}$	$\bar{\tau}_{zx}^{CR}$	$\bar{\tau}_{zx}^{EE}$	$\bar{\tau}_{yz}^{CR}$	$\bar{\tau}_{yz}^{EE}$
4	1	Present	0.0191	0.0011	0.0011	0.0039	0.0026	0.0035	0.0026	0.0035
		HSDT [3]	0.0197	0.0010	0.0010	0.0031	0.0029	0.0028	0.0029	0.0028
		FSDT [2]	0.0190	0.0010	0.0010	0.0015	0.0022	0.0033	0.0022	0.0033
		CPT [1]	0.0153	0.0010	0.0010	0.0015	---	0.0033	---	0.0033
	3	Present	0.0148	0.0008	0.0008	0.0037	0.0023	0.0033	0.0023	0.0033
		HSDT [3]	0.0149	0.0007	0.0007	0.0030	0.0026	0.0025	0.0026	0.0025
		FSDT [2]	0.0146	0.0007	0.0007	0.0013	0.0020	0.0030	0.0020	0.0030
		CPT [1]	0.0126	0.0007	0.0007	0.0013	---	0.0030	---	0.0030
	5	Present	0.0053	0.0002	0.0002	0.0034	0.0015	0.0029	0.0015	0.0029
		HSDT [3]	0.0050	0.0001	0.0001	0.0026	0.0018	0.0020	0.0018	0.0020
		FSDT [2]	0.0051	0.0002	0.0002	0.0010	0.0015	0.0022	0.0015	0.0022
		CPT [1]	0.0053	0.0002	0.0002	0.0010	---	0.0022	---	0.0022
10	1	Present	0.0159	0.0010	0.0010	0.0019	0.0032	0.0027	0.0032	0.0027
		HSDT [3]	0.0160	0.0010	0.0010	0.0020	0.0032	0.0030	0.0032	0.0030
		FSDT [2]	0.0159	0.0010	0.0010	0.0015	0.0022	0.0033	0.0022	0.0033
		CPT [1]	0.0153	0.0010	0.0010	0.0015	---	0.0033	---	0.0033
	3	Present	0.0129	0.0008	0.0008	0.0018	0.0029	0.0024	0.0029	0.0024
		HSDT [3]	0.0130	0.0007	0.0007	0.0018	0.0029	0.0027	0.0029	0.0027
		FSDT [2]	0.0129	0.0007	0.0007	0.0013	0.0020	0.0030	0.0020	0.0030
		CPT [1]	0.0126	0.0007	0.0007	0.0013	---	0.0030	---	0.0030
	5	Present	0.0053	0.0002	0.0002	0.0015	0.0022	0.0019	0.0022	0.0019
		HSDT [3]	0.0053	0.0002	0.0002	0.0015	0.0022	0.0020	0.0022	0.0020
		FSDT [2]	0.0053	0.0002	0.0002	0.0010	0.0015	0.0022	0.0015	0.0022
		CPT [1]	0.0053	0.0002	0.0002	0.0010	---	0.0022	---	0.0022
100	1	Present	0.0153	0.0010	0.0010	0.0015	0.0034	0.0033	0.0034	0.0033
		HSDT [3]	0.0153	0.0010	0.0010	0.0016	0.0033	0.0033	0.0033	0.0033
		FSDT [2]	0.0153	0.0010	0.0010	0.0015	0.0022	0.0033	0.0022	0.0033
		CPT [1]	0.0153	0.0010	0.0010		---	0.0033	---	0.0033
	3	Present	0.0125	0.0008	0.0008	0.0013	0.0031	0.0030	0.0031	0.0030
		HSDT [3]	0.0126	0.0007	0.0007	0.0015	0.0030	0.0030	0.0030	0.0030
		FSDT [2]	0.0126	0.0007	0.0007	0.0013	0.0020	0.0030	0.0020	0.0030
		CPT [1]	0.0126	0.0007	0.0007	0.0013	---	0.0030	---	0.0030
	5	Present	0.0053	0.0002	0.0002	0.0010	0.0024	0.0023	0.0024	0.0023
		HSDT [3]	0.0053	0.0002	0.0002	0.0012	0.0023	0.0023	0.0023	0.0023
		FSDT [2]	0.0053	0.0002	0.0002	0.0010	0.0015	0.0022	0.0015	0.0022
		CPT [1]	0.0053	0.0002	0.0002	0.0010	---	0.0022	---	0.0022

**Table 7.** Comparison of non-dimensional deflection and stresses in isotropic square plate subjected to central concentrated load

<i>S</i>	<i>K</i>	Theory	$\bar{w}$	$\bar{\sigma}_x$	$\bar{\sigma}_y$	$\bar{\tau}_{xy}$	$\bar{\tau}_{zx}^{CR}$	$\bar{\tau}_{zx}^{EE}$	$\bar{\tau}_{yz}^{CR}$	$\bar{\tau}_{yz}^{EE}$
4	1	Present	21.709	11.950	11.950	0.3647	0.6488	1.3790	0.6488	1.3790
		HSDT [3]	20.831	6.7873	6.7873	0.3660	0.7585	1.1278	0.7585	1.1278
		FSDT [2]	20.498	2.3435	2.3435	0.3645	0.6652	0.9978	0.6652	0.9978
		CPT [1]	11.564	2.3442	2.3442	0.3648	---	0.9985	---	0.9985
	3	Present	19.014	11.738	11.738	0.2797	0.4577	1.2807	0.4577	1.2807
		HSDT [3]	17.773	6.5913	6.5913	0.2713	0.5619	1.0253	0.5619	1.0253
		FSDT [2]	17.674	2.1695	2.1695	0.2773	0.5377	0.8065	0.5377	0.8065
		CPT [1]	9.8169	2.2071	2.2071	0.2934	---	0.8399	---	0.8399
	5	Present	12.658	11.154	11.154	0.0931	0.0542	1.0742	0.0542	1.0742
		HSDT [3]	10.941	6.1075	6.1075	0.0756	0.1697	0.8220	0.1697	0.8220
		FSDT [2]	11.203	1.7483	1.7483	0.0895	0.2740	0.4110	0.2740	0.4110
		CPT [1]	5.2137	1.8364	1.8364	0.1090	---	0.4376	---	0.4376
10	1	Present	13.087	5.2258	5.2258	0.3646	0.7933	1.0504	0.7933	1.0504
	HSDT [3]	13.222	3.4420	3.4420	0.3526	0.9149	0.8035	0.9149	0.8035	

		FSDT [2]	12.994	2.3441	2.3441	0.3647	0.6656	0.9983	0.6656	0.9983
		CPT [1]	11.564	2.3442	2.3442	0.3648	---	0.9985	---	0.9985
	3	Present	11.218	5.0726	5.0726	0.2914	0.6260	0.9659	0.6260	0.9659
		HSDT [3]	11.287	3.2959	3.2959	0.2776	0.7499	0.6826	0.7499	0.6826
		FSDT [2]	11.090	2.2008	2.2008	0.2907	0.5562	0.8343	0.5562	0.8343
		CPT [1]	9.8169	2.2071	2.2071	0.2934	---	0.8399	---	0.8399
	5	Present	6.3915	4.6614	4.6614	0.1069	0.2130	0.7572	0.2130	0.7572
		HSDT [3]	6.3405	2.9086	2.9086	0.0917	0.3483	0.4352	0.3483	0.4352
		FSDT [2]	6.2013	1.8209	1.8209	0.1053	0.2883	0.4324	0.2883	0.4324
		CPT [1]	5.2137	1.8364	1.8364	0.1090	---	0.4376	---	0.4376
100	1	Present	11.542	2.5076	2.5076	0.3636	1.0259	0.9842	1.0259	0.9842
		HSDT [3]	11.584	2.3569	2.3569	0.3502	0.9974	0.9949	0.9974	0.9949
		FSDT [2]	11.575	2.3439	2.3439	0.3647	0.6655	0.9982	0.6655	0.9982
		CPT [1]	11.564	2.3442	2.3442	0.3648	---	0.9985	---	0.9985
	3	Present	9.8035	2.3623	2.3623	0.2926	0.8632	0.8277	0.8632	0.8277
		HSDT [3]	9.8340	2.2197	2.2197	0.2788	0.8388	0.8362	0.8388	0.8362
		FSDT [2]	9.8275	2.2068	2.2068	0.2932	0.5597	0.8397	0.5597	0.8397
		CPT [1]	9.8169	2.2071	2.2071	0.2934	---	0.8399	---	0.8399
	5	Present	5.2156	1.9688	1.9688	0.1089	0.4496	0.4298	0.4496	0.4298
		HSDT [3]	5.2259	1.8487	1.8487	0.0954	0.4365	0.4338	0.4365	0.4338
		FSDT [2]	5.2231	1.8362	1.8362	0.1089	0.2917	0.4375	0.2917	0.4375
		CPT [1]	5.2137	1.8364	1.8364	0.1090	---	0.4376	---	0.4376

## 5. Conclusions

A trigonometric plate theory is assessed for bending analysis of square isotropic plates resting on Winkler elastic foundation subjected to various static loadings. The theory is variationally consistent and obviates the need of shear correction factor. The displacements and stresses are obtained for different foundation moduli. The present results are compared with those generated using other theories. From the numerical results and discussion, the following conclusions are drawn.

1. The results of displacements and stresses predicted by the present theory are in excellent agreement with those of Reddy's theory.
  2. The transverse displacements and stresses are found to decrease with an increase in foundation modulus.
- The present theory can predict the effect of local stress concentration on the in-plane and transverse shear stress distributions due to concentrated load more prominently compared with other higher order theories.

## References

- [1] Kirchhoff, G.R., Uber das gleichgewicht und die bewegung einer elastischen Scheibe, *Journal for Pure and Applied Mathematics*, 40, 1850, 51-88.
- [2] Mindlin, R.D., Influence of rotatory inertia and shear on flexural motions of isotropic, elastic plates, *Journal of Applied Mechanics*, 18, 1951, 31-38.
- [3] Reddy, J.N., A simple higher order theory for laminated composite plates, *Journal of Applied Mechanics*, 51, 1984, 745-752.
- [4] Matsunaga, H., Vibration and stability of thick plates on elastic foundations, *Journal of Engineering Mechanics*, 126(1), 2000, 27-34.
- [5] Huang, M.H., Thambiratnam, D.P., Analysis of plate resting on elastic supports and elastic foundation by finite strip method, *Computers and Structures*, 79(29-30), 2001, 2547-2557.
- [6] Chen, W.Q., Bian, Z.G., A mixed method for bending and free vibration of beams resting on a Pasternak elastic foundation, *Applied Mathematical Modelling*, 28(10), 2004, 877-890.
- [7] Atmane, H.A., Tounsi, A., Mechab, I., Bedia, E.A.A., Free vibration analysis of functionally graded plates resting on Winkler-Pasternak elastic foundations using a new shear deformation theory, *International Journal of Mechanics and Materials in Design*, 6(2), 2010, 113-121.
- [8] Thai, H.T., Park, M., Choi, D.H., A simple refined theory for bending, buckling, and vibration of thick plates resting on elastic foundation, *International Journal of Mechanical Science*, 73, 2013, 40-52.
- [9] Zenkour, A.M., Bending of orthotropic plates resting on Pasternak's foundations by mixed shear deformation theory, *Acta Mechanica Sinica*, 27(6), 2011, 956-962.
- [10] Zenkour, A.M., Allam, M.N.M., Shaker, M.O., Radwan, A.H., On the simple and mixed first-order theories for plates resting on elastic foundations, *Acta Mechanica*, 220(1-4), 2011, 33-46.
- [11] Sayyad, A.S., Flexure of thick orthotropic plates by exponential shear deformation theory, *Latin American Journal of Solids and Structures*, 10, 2013, 473-490.

- [12] Akbas, S.D., Vibration and static analysis of functionally graded porous plates, *Journal of Applied and Computational Mechanics*, 3(3), 2017, 199-207.
- [13] Akbas, S.D., Stability of a non-homogenous porous plate by using generalized differential quadrature method, *International Journal of Engineering & Applied Sciences*, 9(2), 2017, 147-155.
- [14] Akbas, S.D., Static analysis of a nano plate by using generalized differential quadrature method, *International Journal of Engineering & Applied Sciences*, 8(2), 2016, 30-39.
- [15] Civalek, O., Analysis of thick rectangular plates with symmetric cross-ply laminates based on first-order shear deformation theory, *Journal of Composite Materials*, 42(26), 2008, 2853-2867.
- [16] Gurses, M., Civalek, O., Korkmaz, A.K., Ersoy, H., Free vibration analysis of symmetric laminated skew plates by discrete singular convolution technique based on first-order shear deformation theory, *International Journal for Numerical Methods in Engineering*, 79, 2009, 290–313.
- [17] Sayyad, A.S., Ghugal, Y.M., On the free vibration analysis of laminated composite and sandwich plates: A review of recent literature with some numerical results, *Composite Structures*, 129, 2015, 177–201.
- [18] Sayyad, A.S., Ghugal, Y.M., Bending, buckling and free vibration of laminated composite and sandwich beams: A critical review of literature, *Composite Structures*, 171, 2017, 486–504.
- [19] Ghugal, Y.M., Sayyad, A.S., A static flexure of thick isotropic plates using trigonometric shear deformation theory, *Journal of Solid Mechanics*, 2(1), pp. 79-90, 2010.
- [20] Ghugal, Y.M., Sayyad, A.S., Free vibration of thick isotropic plates using trigonometric shear deformation theory, *Journal of Solid Mechanics*, 3(2), 2011, 172-182.
- [21] Ghugal, Y.M., Sayyad, A.S., Static flexure of thick orthotropic plates using trigonometric shear deformation theory, *Journal of Structural Engineering*, 39(5), 2013, 512-521.
- [22] Ghugal, Y.M., Sayyad, A.S., Free vibration of thick orthotropic plates using trigonometric shear deformation theory, *Latin American Journal of Solids and Structures*, 8, 2011, 229-243.
- [23] Timoshenko, S.P., Goodier, J.M., *Theory of Elasticity*, McGraw-Hill, Singapore, 1970.